Sensing prokaryotic mRNA signifies microbial viability and promotes immunity

Leif E. Sander, Michael J. Davis, Mark V. Boekschoten, Derk Amsen, Christopher C. Dascher, Bernard Ryffel, Joel A. Swanson, Michael Müller and J. Magarian Blander

Supplementary Figures 1-22

Supplementary Figure 1

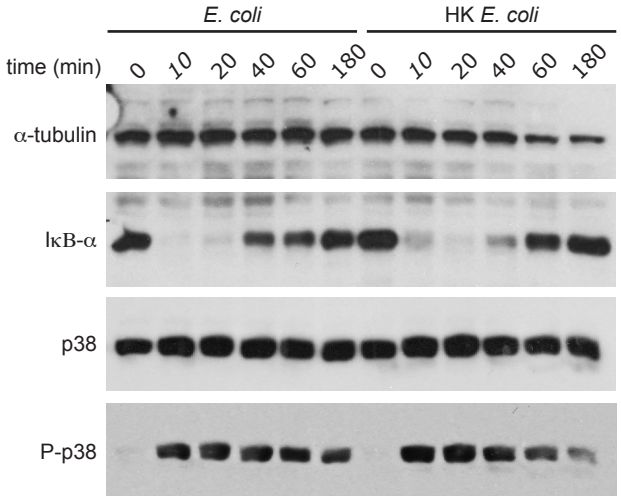

Supplementary Fig. 1. Viable and heat killed *E. coli* induce NF-κB and MAPK activation. Bone marrow derived macrophages (BMM) were stimulated with viable or heat killed (HK) *ThyA⁻ E. coli* for the indicated times. Cellular lysates were immunoblotted and probed for the indicated proteins. As a readout for NF-κB activation, IκB-α degradation was observed 10 minutes post stimulation with either viable or HK *ThyA⁻ E. coli* , and its re-synthesis restored detection at 40 minutes. MAPK activation was assessed by examining the phosphorylation of p38 (P-p38) which was detected beginning at 10 minutes after stimulation with either viable or HK *ThyA⁻ E. coli*.

Supplementary Figure 2

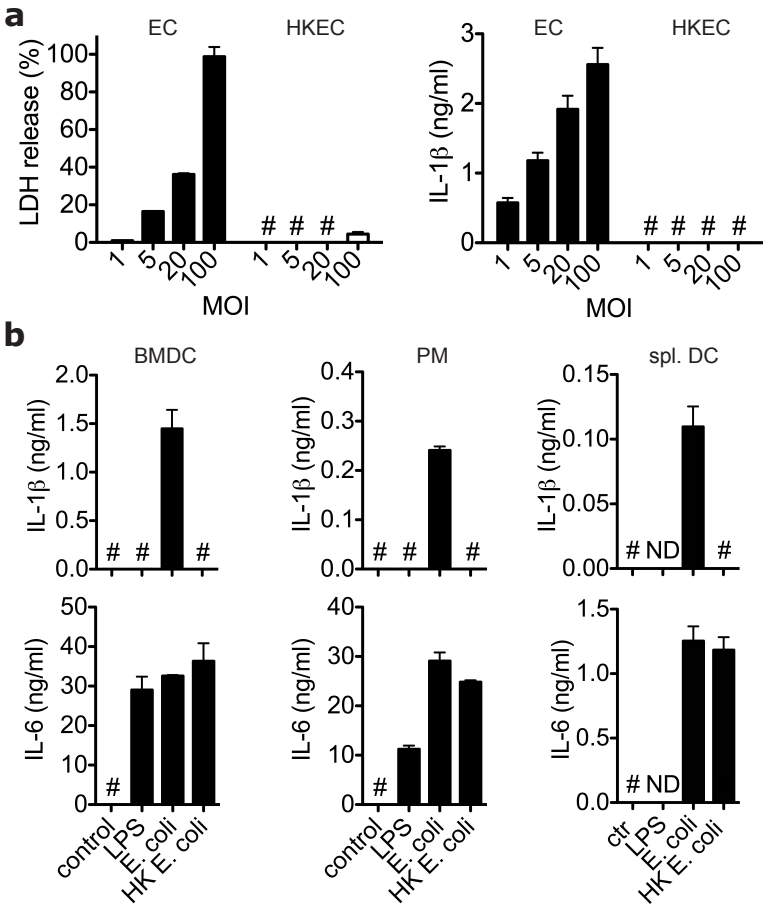

Supplementary Fig. 2. Viability-induced responses are dose-dependent and not restricted to BMM. (**a**) BMM were stimulated with viable or heat killed (HK) *ThyA*$^{-}$ *E. coli* at the indicated multiplicities of infection (MOI) for 24 hours. (**b**) Bone marrow derived dendritic cells (BMDC), peritoneal macrophages (PM) and splenic DC (spl. DC) were incubated with LPS (100ng/ml), viable or heat killed (HK) *ThyA*$^{-}$ *E. coli* for 24 hours. Lactate dehydrogenase (LDH), IL-1β and IL-6 production were measured in the supernatants. by ELISA. #; 'not detected', ND; not determined. All bars represent mean ± s.e.m.

Supplementary Figure 3

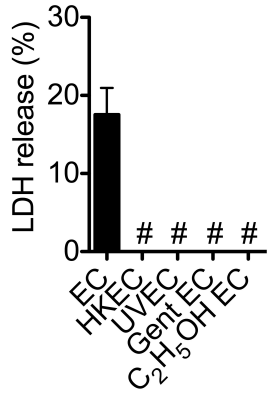

Supplementary Fig. 3. Viable but not killed bacteria induce pyroptosis irrespective of mode of death. BMM were incubated with viable *ThyA⁻ E. coli* (EC) or *ThyA⁻ E. coli* killed by various means prior to addition to BMM. *ThyA⁻ E. coli* were killed by heat (HKEC), UV irradiation (UVEC), treatment with Gentamicin sulfate (Gent EC), or 70% Ethanol (C_2H_5OH EC). LDH release was measured in the supernatant 24 hours later. #; 'not detected'.

Supplementary Figure 4

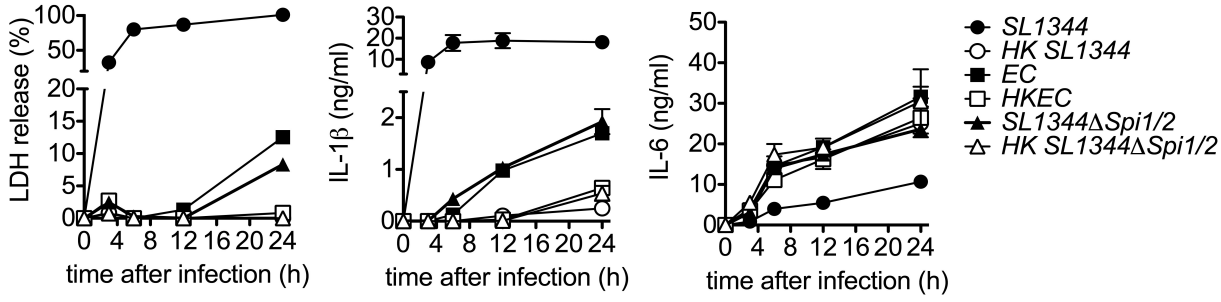

Supplementary Fig. 4. Different magnitude and kinetics of pyroptosis and IL-1β production in response to viability *versus* virulence factors. BMM were incubated with the indicated bacteria for the indicated times, and pyroptosis (LDH release, left), IL-1β (middle) and IL-6 production (right) were measured. SL1344 is a wild type (*wt*) strain of *S. typhimurium*; SL1344ΔSpi1/2 is a mutant lacking the *Salmonella* pathogenicity island (SPI) 1 and SPI 2 T3SS. LDH and IL-1β release were observed in response to both avirulent viable *ThyA⁻ E. coli* and SL1344ΔSpi1/2 indicating a trigger other than virulence factors. On the other hand, *wt S. typhimurium* induced high levels of LDH and IL-1β release within 3 hours, known to be T3SS dependent in this case (compare to levels with T3SS mutant SL1344ΔSpi1/2). IL-6 levels were comparable in response to all bacteria except as expected for SL1344, where survival of the BMM was compromised.

Supplementary Figure 5

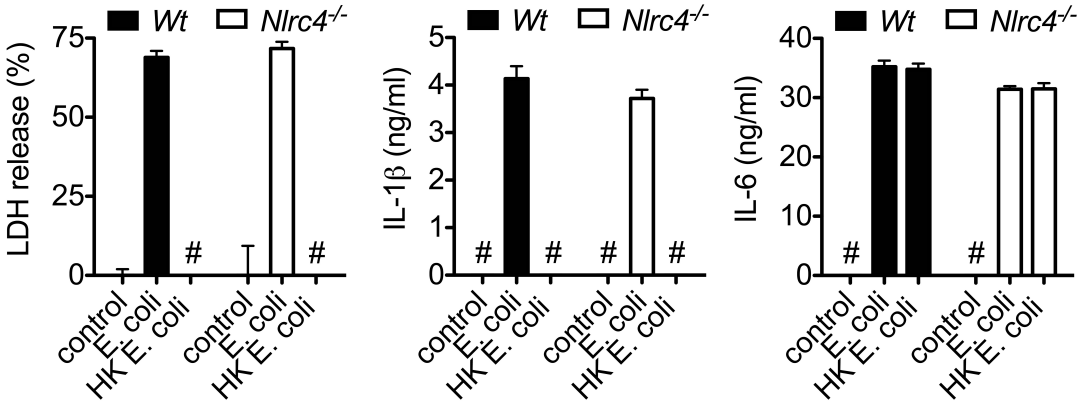

Supplementary Fig. 5. Pyroptosis and IL-1β secretion induced by viable avirulant *E. coli* are independent of the Nod-like receptor NLRC4. BMDC derived from *wt* or *Nlrc4*$^{-/-}$ mice were incubated with viable or heat killed (HK) *ThyA*$^{-}$ *E. coli*. Cell culture supernatants were harvested after 24 hours and pyroptosis was determined by measurement of LDH release. IL-1β and IL-6 secretion was measured by ELISA. #; 'not detected'.

Supplementary Figure 6

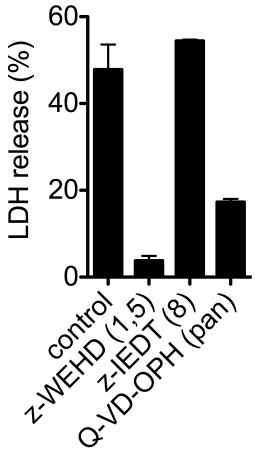

Supplementary Fig. 6. Pyroptosis induced by *E. coli* is mediated by caspase-1 and is independent of caspase-8. BMM were incubated with viable *ThyA*$^{-}$ *E. coli* and the indicated caspase inhibitors. The specificities of inhibitors z-WEHD, z-IEDT and Q-VD-OPH to various caspases are indicated in parentheses. Pyroptosis was determined by measurement of LDH release at 24 hours.

Supplementary Figure 7

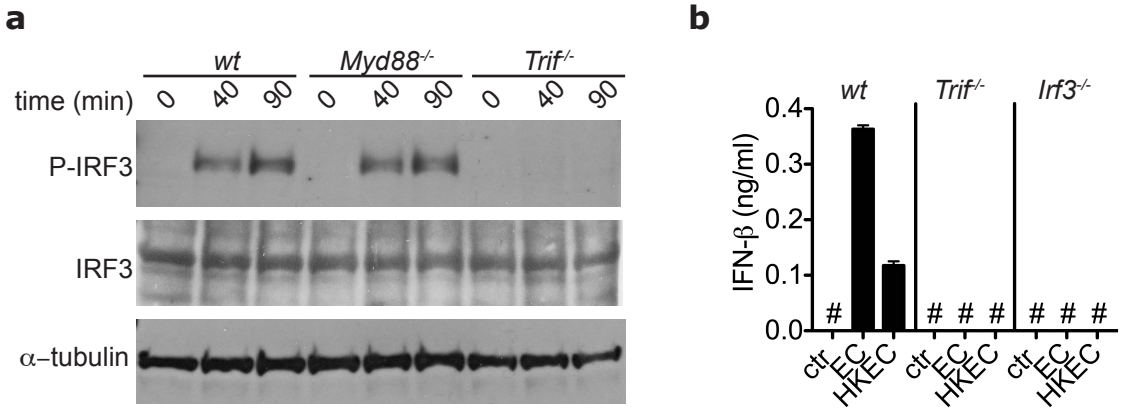

Supplementary Fig. 7. IFN-β production induced by viable *E. coli* is dependent on TRIF-IRF3 signalling. **(a)** BMM derived from *wt*, *Myd88*$^{-/-}$ or *Trif*$^{-/-}$ mice were incubated with viable *ThyA*$^{-}$ *E. coli* for the indicated times. Cell lysates were immunoblotted and probed for phosphorylated IRF3 (P-IRF3), total IRF3 and α–tubulin as indicated. **(b)** BMM derived from *wt*, *Trif*$^{-/-}$ or *Irf3*$^{-/-}$ mice were incubated with viable *ThyA*$^{-}$ *E. coli* (EC) or heat killed (HK) *ThyA*$^{-}$ *E. coli* (HKEC) or medium alone (ctr). IFN-β production was measured in supernatants after 24 hours by ELISA. **#**; 'not detected'.

Supplementary Figure 8

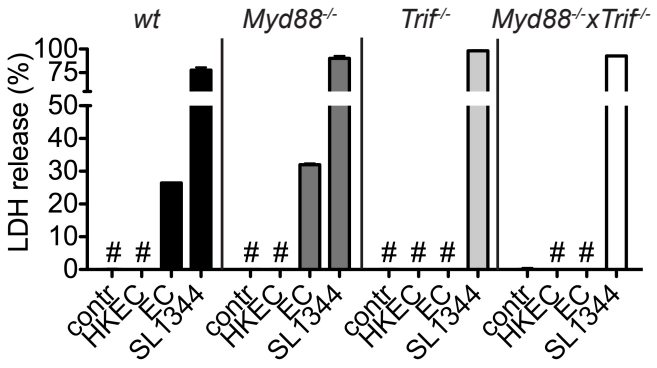

Supplementary Fig. 8. *S. typhimurium* induces pyroptosis in macrophages independently of TLR signalling. BMM derived from *wt*, *Myd88*$^{-/-}$, *Trif*$^{-/-}$ or *Myd88*$^{-/-}$*xTrif*$^{-/-}$ mice were incubated with viable *ThyA*$^{-}$ *E. coli* (EC), heat killed (HK) *ThyA*$^{-}$ *E. coli* (HKEC) or viable *S. typhimurium* (SL1344) for 24 hours and LDH release was measured. **#**; 'not detected'.

Supplementary Figure 9

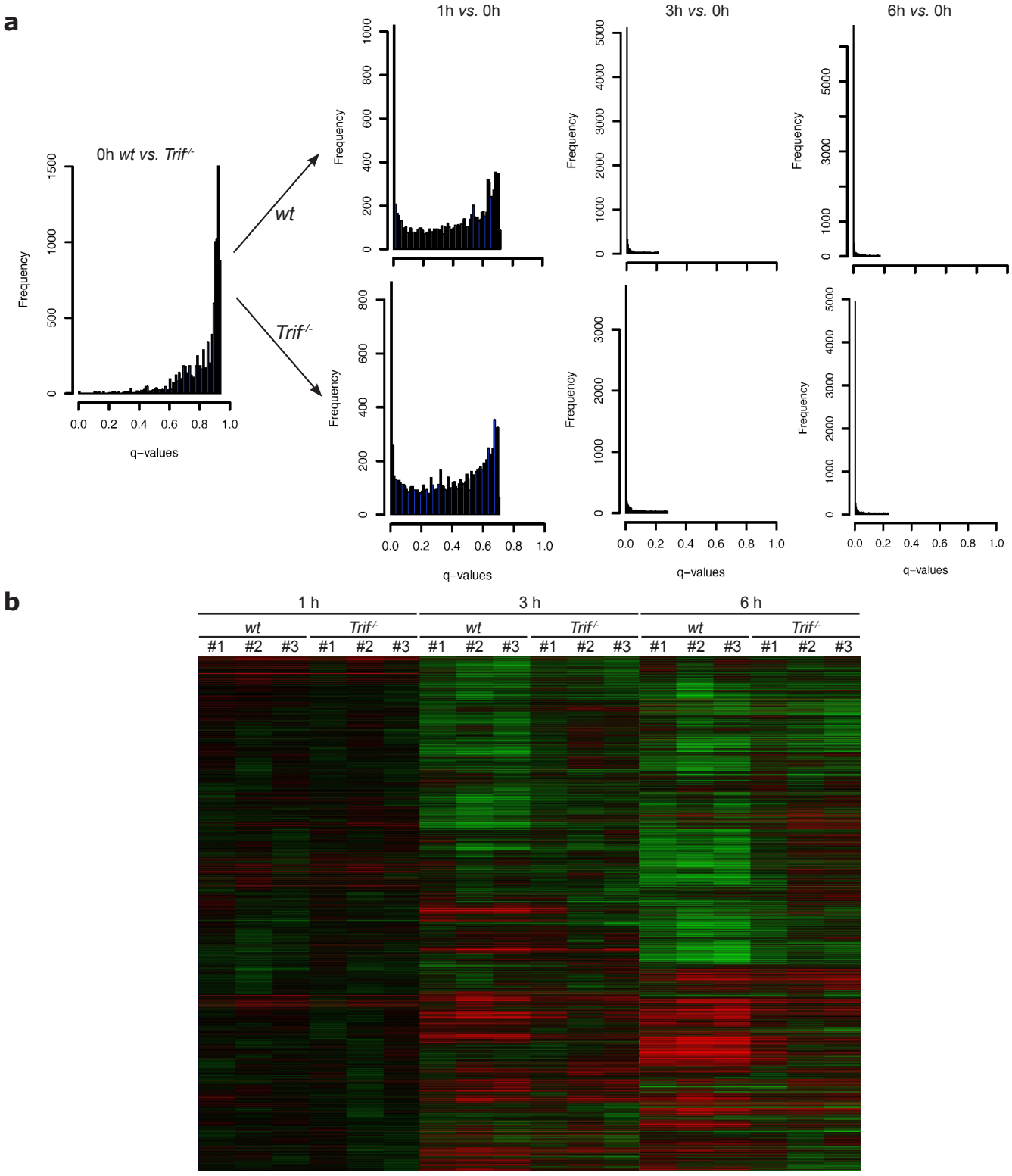

Supplementary Fig. 9. Genome-wide transcriptional profile of *wt* and *Trif*$^{-/-}$ BMM at various time points after phagocytosis of viable avirulent *E. coli*. BMM derived from *wt* or *Trif* $^{-/-}$ mice were incubated with viable *ThyA*$^{-}$ *E. coli* at a MOI of 20 for the indicated time points. RNA was extracted and subjected to transcriptional analysis by Affymetrix gene microarray. The results of three independent experiments is shown. (**a**) IBMT q-value distribution comparing gene expression in *wt* and *Trif*$^{-/-}$ BMM at steady state (far left '0h *wt vs. Trif*$^{-/-}$') and for *wt* and *Trif*$^{-/-}$ BMM individually at 1, 3 and 6 hours after phagocytosis of *ThyA*$^{-}$ *E. coli*. These results illustrate that there are no major differences in gene expression of *wt* and *Trif*$^{-/-}$ BMM at steady state, and that both *wt* and *Trif*$^{-/-}$ BMM rapidly induce a strong transcriptional response after uptake of *E. coli* as evidenced by a shift to low q-values in both genotypes. (**b**) Transcriptional profile of 9922 genes is shown in a heat map.

Supplementary Figure 10

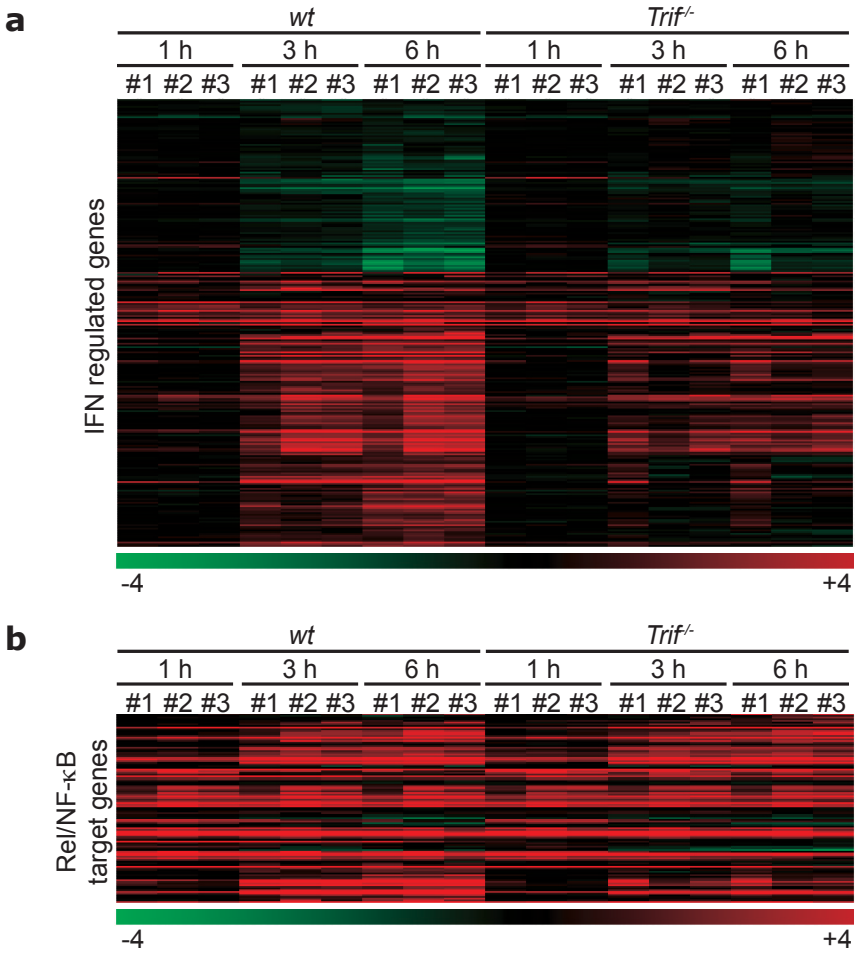

Supplementary Fig. 10. Expression of IFN-regulated genes and Rel/NF-κB target genes in *wt* and *Trif*$^{-/-}$ BMM at various time points after phagocytosis of viable avirulent *E. coli*. BMM derived from *wt* or *Trif* $^{-/-}$ mice were incubated with viable *ThyA*$^{-}$ *E. coli* at a MOI of 20 for the indicated time points. RNA was extracted and subjected to transcriptional analysis by Affymetrix gene microarray. The results of three independent experiments numbered 1, 2 and 3 are shown. Heat maps of (**a**) IFN-regulated genes and (**b**) Rel/NF-κB target genes.

Supplementary Figure 11

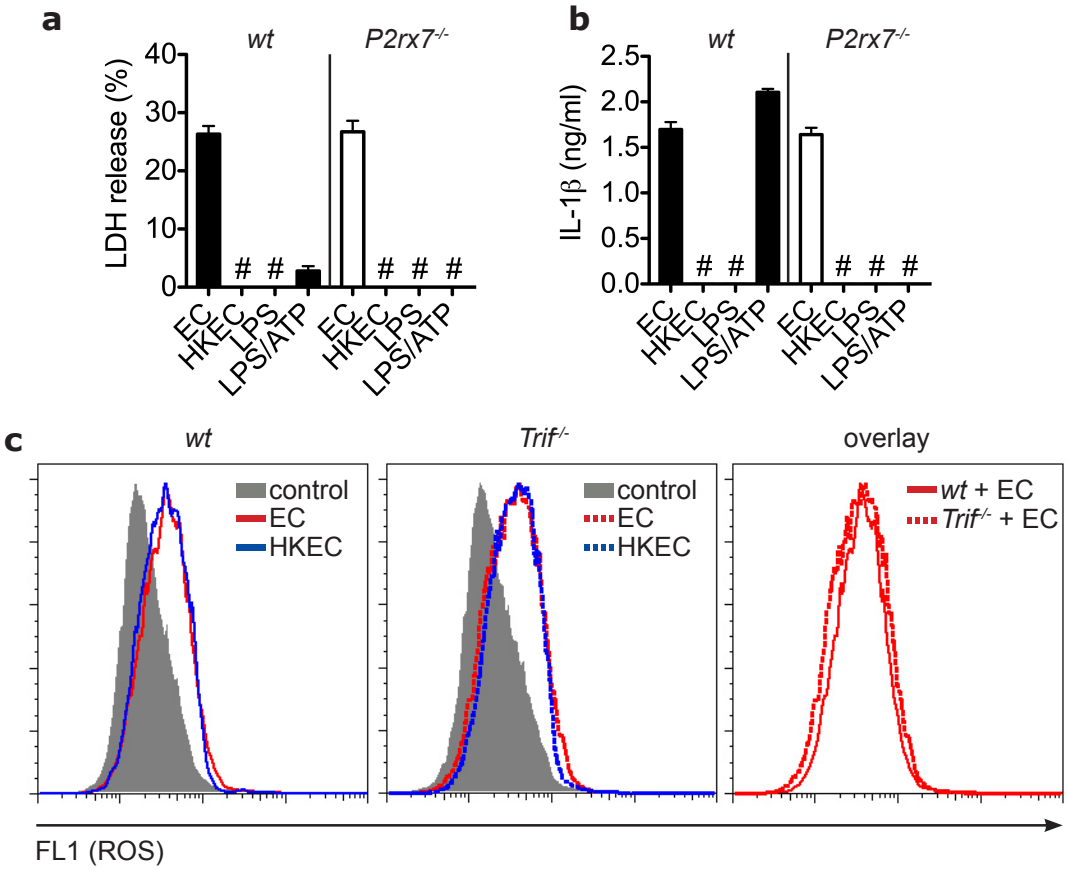

Supplementary Fig. 11. Pyroptosis and IL-1β production induced by viable avirulent *E. coli* is independent of activation of the P_2X_7R, and TRIF is dispensable for ROS production. BMM derived from *wt* or *P2rx7*$^{-/-}$ mice were incubated with the indicated stimuli for 24 hours and pyroptosis **(a)** and IL-1β production **(b)** were measured. While viable *ThyA*$^{-}$ *E. coli* induce significant release of LDH and IL-1β in *wt* and *P2rx7*$^{-/-}$ cells, LPS+ATP-induced pyroptosis and IL-1β production are abrogated in *P2rx7*$^{-/-}$ BMM. (**c**) BMM derived from *wt* or *Trif* $^{-/-}$ mice were pulsed with the cell permeable ROS indicator H2DCFDA, washed and then incubated with the indicated stimuli for 1 hour and washed again. ROS production was measured by flow cytometry. **#**; 'not detected'.

Supplementary Figure 12

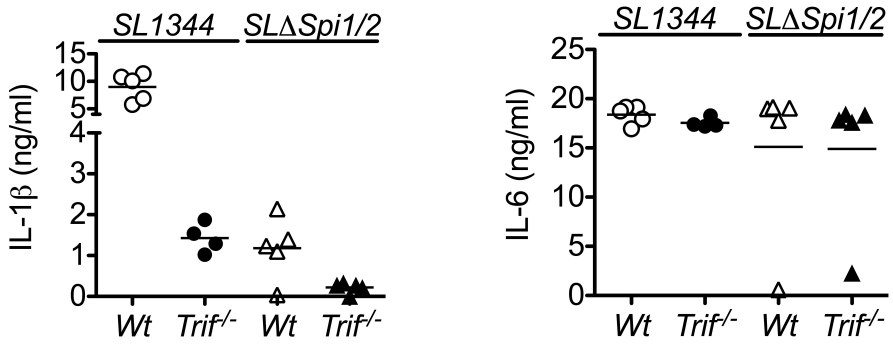

Supplementary Fig. 12. TRIF deficiency strongly reduces IL-1β production in response to *wt* and attenuated *S. typhimurium in vivo*. *Wt* and *Trif*$^{-/-}$ mice were infected with $5x10^8$ cfu *wt* (SL1344) or mutant *S. typhimurium* lacking Salmonella pathogenicity island (SPI) 1 and 2 (SLΔSpi1/2) by intraperitoneal injection. Serum levels of IL-1β and IL-6 after 6 hours were determined by ELISA.

Supplementary Figure 13

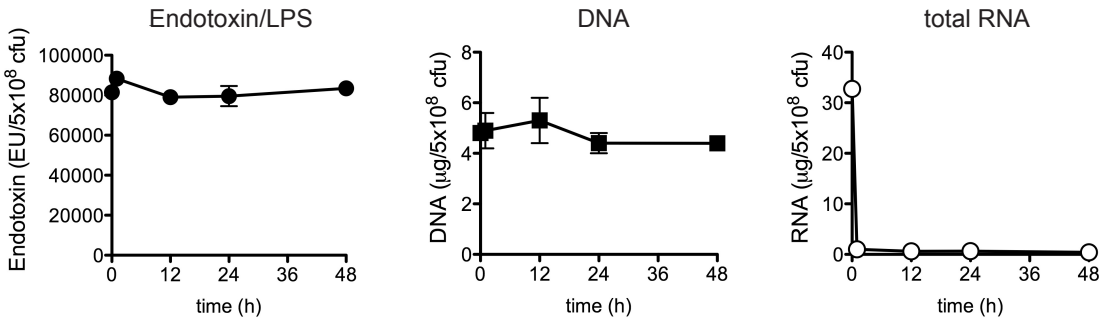

Supplementary Fig. 13. Absolute quantifications of PAMP contents of viable and killed *E. coli.* *ThyA⁻ E. coli* were grown to log phase and either left untreated or subjected to heat killing. Heat killed *ThyA⁻ E. coli* were stored at 4°C for the times indicated and endotoxin/LPS, DNA and total RNA contents were measured as described in the Materials and Methods section.

Supplementary Figure 14

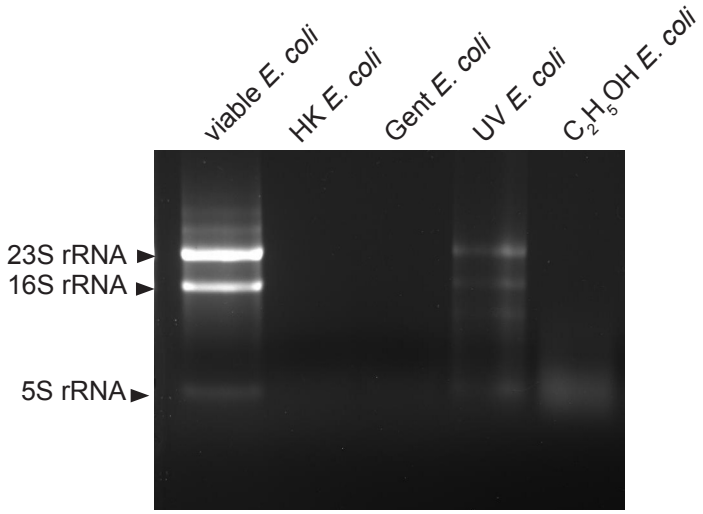

Supplementary Fig. 14. Total RNA contents of viable and killed *E. coli.* *ThyA⁻ E. coli* were grown to log phase and either left untreated or subjected to killing by the indicated method (HK; heat killing at 60°C for 60 minutes, Gent; Gentamicin sulfate treatment for 12 hours, UV; UV irradiation for 10 minutes, C_2H_5OH; 70% Ethanol treatment for 10 minutes followed by washing). Total RNA was extracted from $5x10^8$ bacteria in each case and visualized by 1% agarose gel electrophoresis.

Supplementary Figure 15

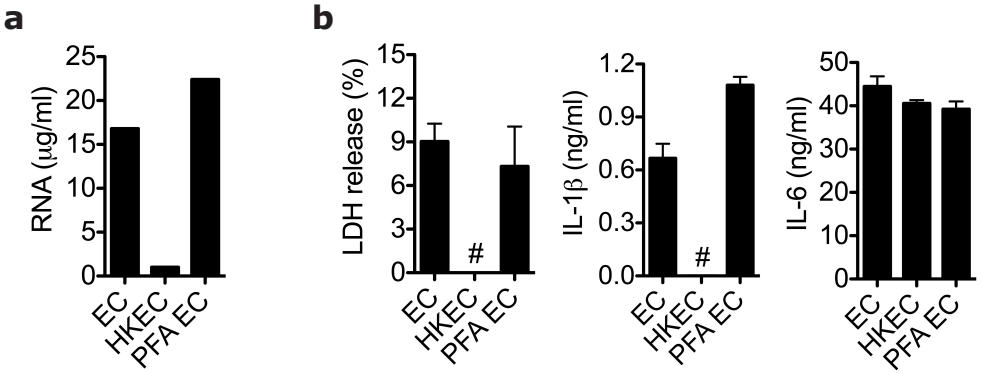

Supplementary Fig. 15. Paraformaldehyde fixation preserves the bacterial RNA content and restores cellular responses. (a) *ThyA⁻ E. coli* were grown to log phase and either left untreated or subjected to heat killing (HK) or paraformaldehyde (PFA) fixation. Total RNA yield extracted from $5x10^8$ bacteria respectively was measured. **(b)** BMM were stimulated with viable, HK or PFA fixed *ThyA⁻ E. coli* for 24 hours. LDH (left) and IL-1β (middle) and IL-6 (right) release were measured in the supernatants. #; 'not detected'.

Supplementary Figure 16

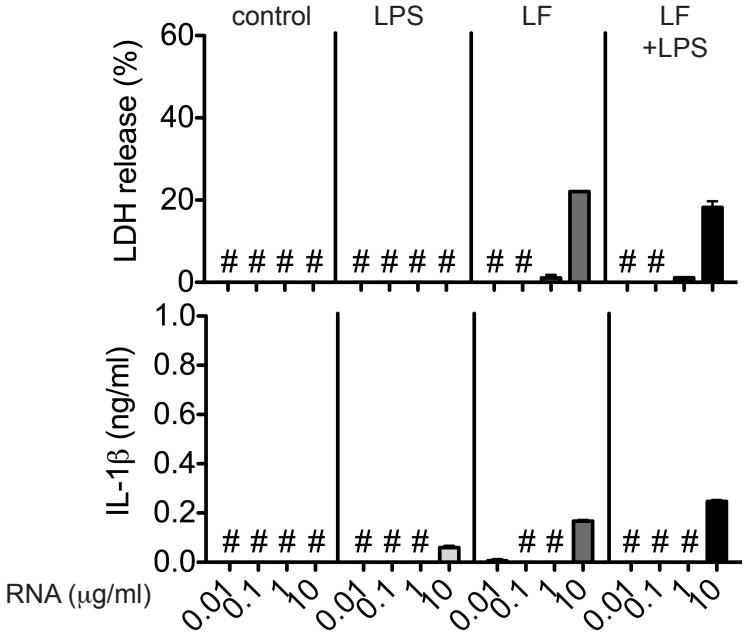

Supplementary Fig. 16. Bacterial RNA alone or in combination with LPS is insufficient to induce inflammasome activation unless delivered directly into the cytosol. BMM were stimulated with total RNA isolated from *ThyA⁻ E. coli* for 24 hours at the indicated concentrations in the presence or absence of LPS and/or Lipofectamine (LF) transfection reagent (Invitrogen). Lipofectamine treatment encapsulates nucleic acids allowing them to cross the plasma membrane and to be released into the cytosol. A combination of LPS and RNA was used to mimic an *E. coli* derived PAMP and RNA. LDH (top) and IL-1β release (bottom) were measured in the supernatants. Note that the LDH and IL-1β levels detected after LF+LPS+RNA treatment are lower than after HK *E. coli* + RNA treatment (Fig. 3c). LPS alone had no effect (data not shown). #; 'not detected'.

Supplementary Figure 17

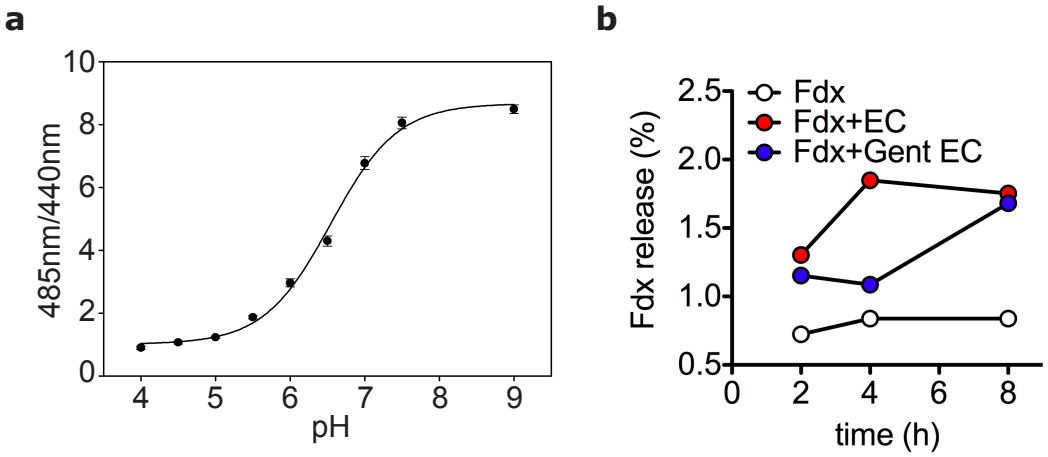

Supplementary Fig. 17. Phagocytosis of *E. coli* induces low level leakage of phagolysosomal contents into the cytosol of BMM. (**a**) Epifluorescence images of fluorescein dextran (Fdx) loaded, permeabilized BMMs were taken at fixed pHs. The ex. 492 nm:ex. 435 ratios were measured and used to generate pH calibration curves (4 parameter sigmoid curve calculated by non-linear regression in sigmaplot). Error bars indicate standard deviations. (**b**) Mean Fdx released into pH neutral compartments relative to total cellular Fdx content was measured in BMMs at the indicated time points after incubation with either medium (Fdx) or viable (Fdx+EC) or gentamicin killed *ThyA*$^{-}$ *E. coli* (Fdx+Gent EC) and expressed as percent Fdx release. Mean was calculated from data shown in Fig. 3f.

Supplementary Figure 18

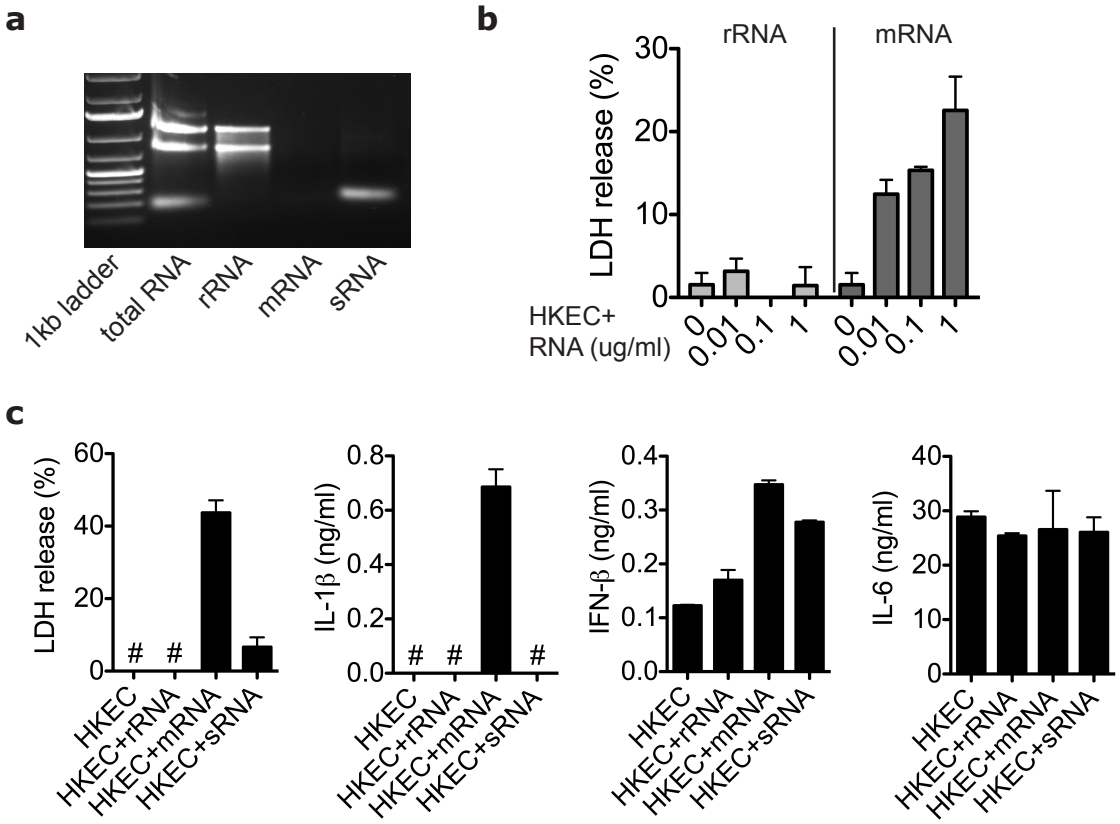

Supplementary Fig. 18. mRNA, but not rRNA, is sufficient to restore inflammasome activation and IFN-β production in response to heat killed *E. coli*. **(a)** Total RNA was extracted from *ThyA*⁻ *E. coli*, fractionated into ribosomal RNA (rRNA), messenger RNA (mRNA) and small RNA (sRNA), and subsequently visualized by 1% agarose gel electrophoresis. **(b)** BMM were incubated with heat killed (HK) *ThyA*⁻ *E. coli* in combination with the indicated doses of purified *E. coli* rRNA (left) or mRNA (right). At 24 hours, pyroptosis was measured as LDH release. (**c**) BMM were incubated with HK *ThyA*⁻ *E. coli* in combination with 0.1μg/ml of the indicated RNA species isolated from *ThyA*⁻ *E. coli*. At 24 hours, pyroptosis was measured as LDH release and IL-1β, IFNβ and IL-6 production were measured by ELISA. #; 'not detected'.

Supplementary Figure 19

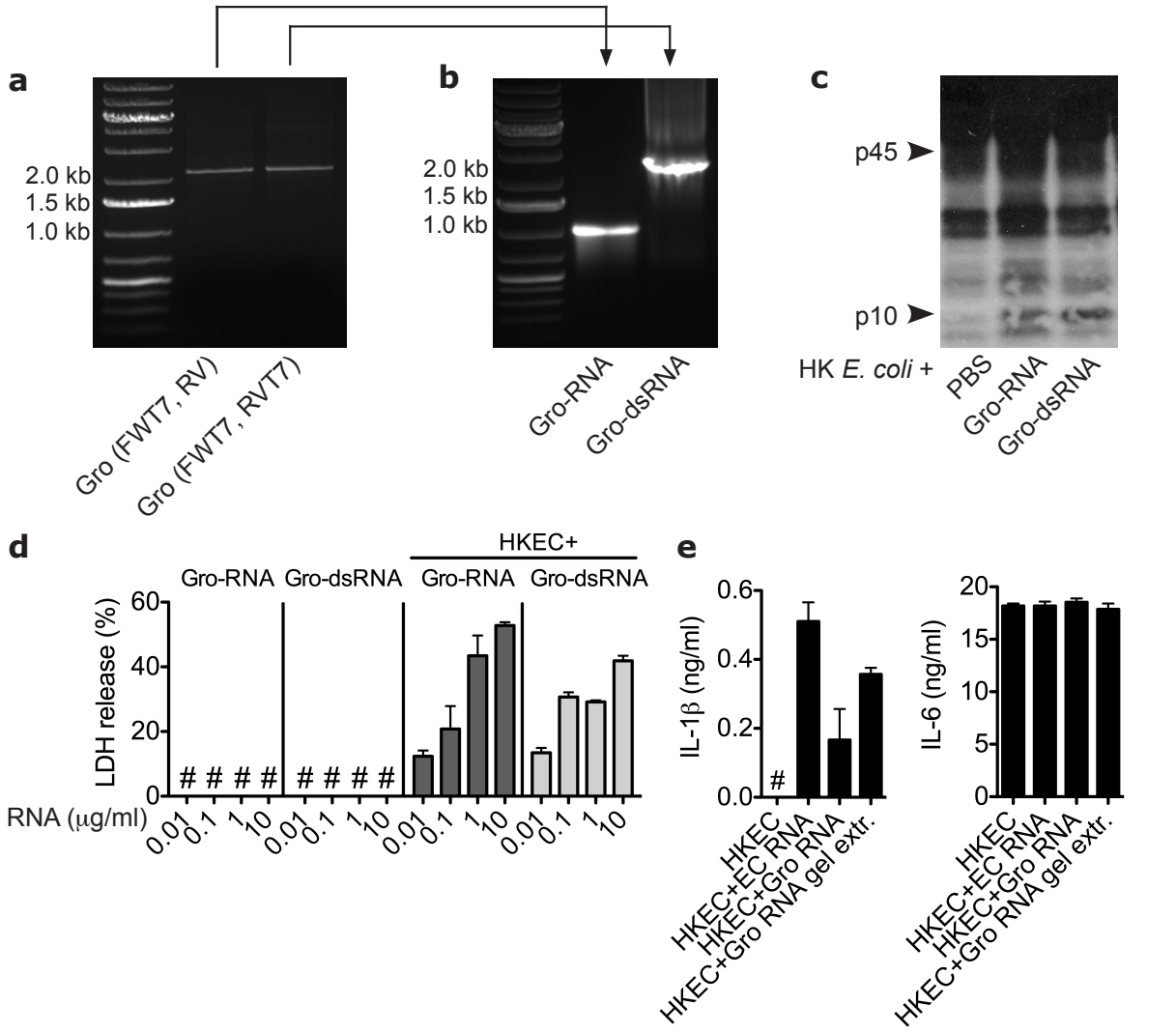

Supplementary Fig. 19. *In vitro* transcribed *E. coli* Gro-mRNA activates the inflammasome only in combination with heat killed *E. coli* and independently of aberrant transcripts. (a) 1% Agarose gel electrophoresis of PCR amplified full-length *E. coli* Gro-operon, using genomic *E. coli* DNA as template, shows a product of 2.1kb. A T7-promotor sequence was introduced in either the sense strand (Gro FWT7, RV) or both the sense and the anti-sense strand (FWT7, RVT7). **(b)** *In vitro* transcription of the PCR product Gro (FWT7, RV) using T7 polymerase yielded Gro-RNA that migrates at 0.95kb, indicating extensive secondary structures resulting in shorter RNA fragments due to base pairing. *In vitro* transcription of Gro (FWT7, RVT7) yields two complementary strands that hybridize, thus do not allow formation of extensive secondary structures and therefore migrate at the predicted size of 2.1kb. **(c)** BMM were incubated with heat killed (HK) *ThyA⁻ E. coli* and the indicated stimuli for 24 hours. Cell lysates were immunoblotted and probed for caspase-1 p10. **(d)** BMM were incubated with increasing concentrations of Gro-RNA or Gro-dsRNA alone or in combination with HK *ThyA⁻ E. coli* for 24 hours, and pyroptosis and IL-1β production (Fig. 4i) were measured. (**e**) In order to rule out the possibility that aberrant transcripts with 3' extensions, frequently observed with T7 polymerase[1], were responsible for the activity of *in vitro* transcribed Gro-RNA, we excised and purified Gro-RNA from agarose gels and added it to BMM (at 10μg/ml) in combination with HK *E. coli*, and measured IL-1β and IL-6 production after 24 hours by ELISA. We compared the activity of gel-extracted Gro-RNA (gel extr.) to regular Gro-RNA and to purified total *E. coli* RNA. **#**; 'not detected'.

1. Cazenave, C. & Uhlenbeck, O.C. RNA template-directed RNA synthesis by T7 RNA polymerase. *Proc Natl Acad Sci U S A* 91, 6972-6976 (1994)

Supplementary Figure 20

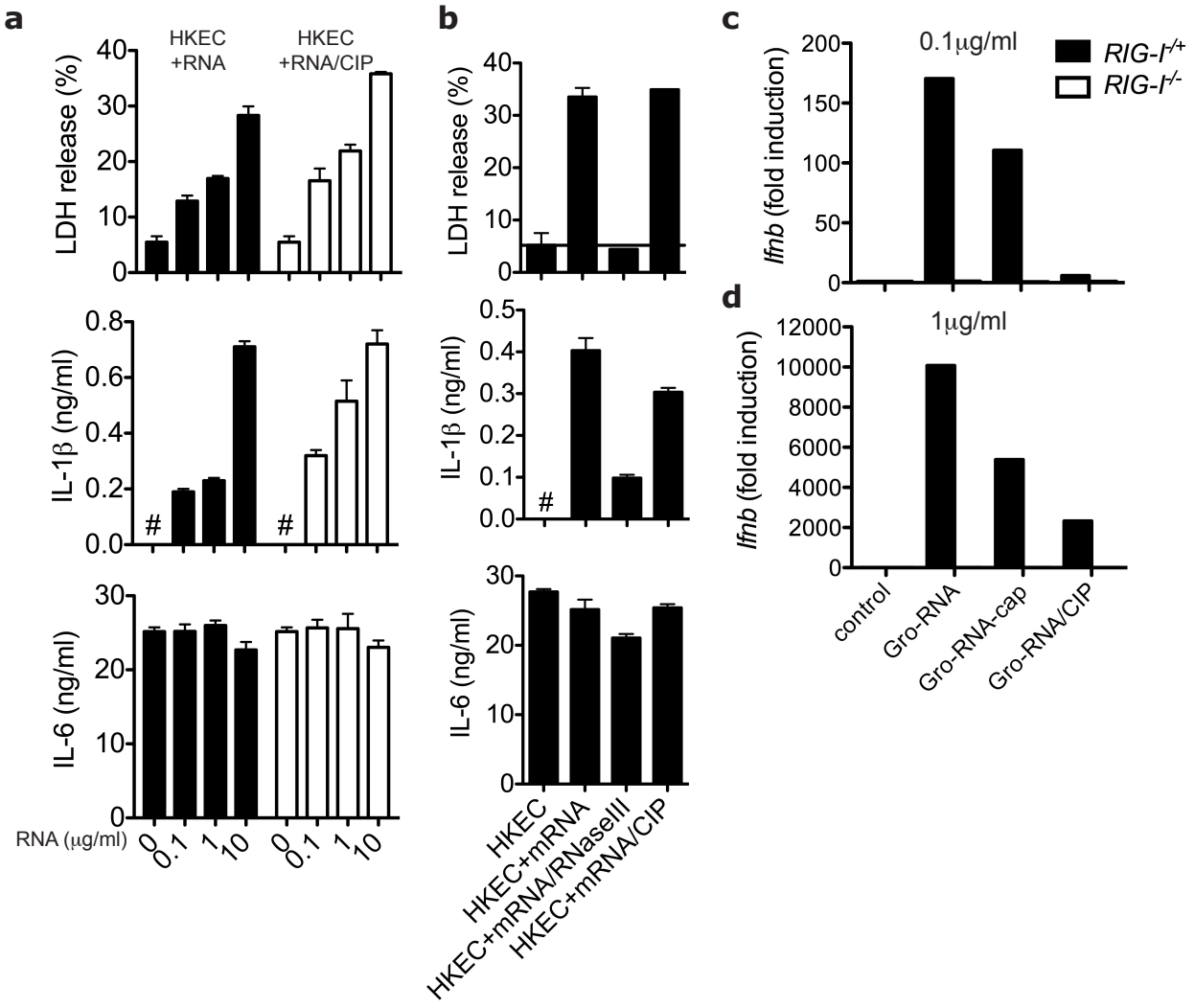

Supplementary Fig. 20. Dephosphorylation of total *E. coli* RNA or purified *E. coli* mRNA does not affect inflammasome activation. (**a**) Total RNA was isolated from viable *ThyA*$^{-}$ *E. coli* and BMM were stimulated with heat killed (HK) *ThyA*$^{-}$ *E. coli* in combination with *E. coli* RNA (HKEC+RNA) or dephosphorylated (CIP treated) *E. coli* RNA (HKEC+RNA/CIP) at the indicated concentrations. (**b**) BMM were stimulated with HK *ThyA*$^{-}$ *E. coli* (HKEC), HK *ThyA*$^{-}$ *E. coli* and 0.1 μg/ml of purified *E. coli* mRNA (HKEC+mRNA), HK *ThyA*$^{-}$ *E. coli* and 0.1 μg/ml of purified *E. coli* mRNA pre-treated with RNase III (HKEC+mRNA/RNaseIII), or HK *ThyA*$^{-}$ *E. coli* and 0.1 μg/ml of dephosphorylated *E. coli* mRNA (HKEC+mRNA/CIP). After 24 hours, pyroptosis (LDH), IL-1β and IL-6 release were measured. **#**; 'not detected'. (**c, d**) Mouse embryonic fibroblasts derived from *RIG-I*$^{-/+}$ or *RIG-I*$^{-/-}$ mice were transfected with *in vitro* transcribed Gro-RNA at 0.1μg/ml **(c)** or 1μg/ml (**d**). IFN-β gene expression 2 hours after transfection was measured by quantitative real time RT-PCR.

Supplementary Figure 21

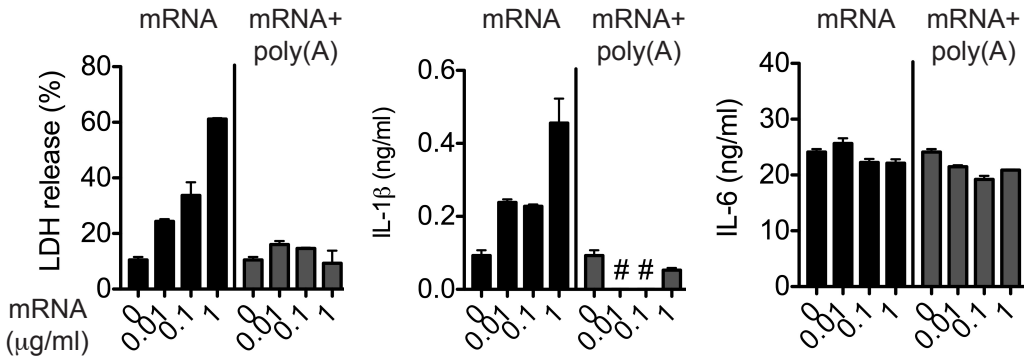

Supplementary Fig. 21. Polyadenylation of *E. coli* mRNA impairs inflammasome activation. mRNA was isolated from total *E. coli* RNA and 3' polyadenylated using *E. coli* poly(A) polymerase (EPAP) (mRNA+poly(A)) or left untreated (mRNA). BMM were then stimulated with heat killed (HK) *ThyA*$^{-}$ *E. coli* alone or in combination with the indicated concentrations of untreated or polyadenylated *E. coli* mRNA. After 24 hours, pyroptosis (LDH release), IL-1β and IL-6 production were measured. **#**; 'not detected'.

Supplementary Figure 22

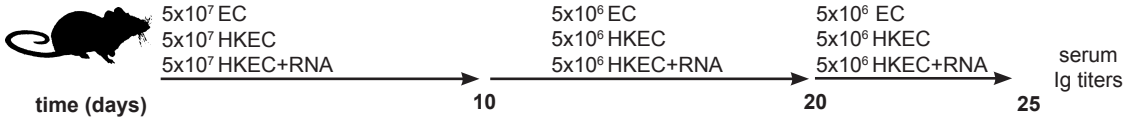

Supplementary Fig. 22. Schematic of vaccination regimen used for immunizations shown in Fig. 4h.